

Inelastic-neutron-scattering study of the spin dynamics in the Haldane-gap system $\text{Ni}(\text{C}_2\text{H}_8\text{N}_2)_2\text{NO}_2\text{ClO}_4$

L. P. Regnault and I. Zaliznyak*

*Département de Recherche Fondamentale sur la Matière Condensée, Service de Physique Statistique, Magnétisme et Supraconductivité,
Laboratoire de Magnétisme et Diffraction Neutronique, Centre d'Etudes Nucléaires, 38054 Grenoble cedex 9, France*

J. P. Renard

Institut d'Electronique Fondamentale, Bâtiment 220, Université de Paris-Sud, 91405 Orsay, France

C. Vettier

European Synchrotron Radiation Facility, Boîte Postale 220, 38043 Grenoble cedex, France

(Received 28 March 1994; revised manuscript received 31 May 1994)

We have investigated the spin dynamics of the nearly ideal one-dimensional $S=1$ antiferromagnet $\text{Ni}(\text{C}_2\text{H}_8\text{N}_2)_2\text{NO}_2\text{ClO}_4$ (NENP) by inelastic neutron scattering. The measurements have been performed as a function of both the wave vector (in the vicinity of the antiferromagnetic point $q=\pi$) and the magnetic field, for field configurations parallel (up to 5 T) or perpendicular to the chain axis (up to 10 T). Our experimental results at low temperature are in good quantitative agreement with most theoretical predictions (both analytical and numerical) established for the spin-1 Haldane-gap system in presence of finite orthorhombic anisotropy: nonmagnetic singlet ground state, three gaps in the excitation spectrum corresponding to the excited triplet ($\Delta_y^0 \approx 1.05$ meV, $\Delta_x^0 \approx 1.23$ meV, $\Delta_z^0 \approx 2.5$ meV), finite correlation lengths at $T=0$ ($\xi_{xy}/d \approx 8$, $\xi_z/d \approx 4$) and unconventional field dependencies. The evolution with field of the various modes and their respective polarization have been determined experimentally and are compared to recent field-theory treatments of the $S=1$ anisotropic antiferromagnetic chain together with numerical calculations on finite-size systems. We present results concerning the field dependencies of the correlation lengths, both in field parallel and perpendicular to the chain axis, which are not fully understood from the existing theories.

I. INTRODUCTION

During the past 20 years one-dimensional magnetic systems have been the subject of numerous theoretical as well as experimental investigations. Such relatively simple systems have been considered since a long time as very important in the understanding of new aspects in statistical physics, like, e.g., nonlinear excitations or many-body quantum effects. More or less, all was thought to be known and understood at the beginning of the 80's. Yet the physics of magnetic one-dimensional systems has been considerably renewed in 1983 by the Haldane conjecture. After Haldane,¹ the low-temperature properties of the one-dimensional Heisenberg antiferromagnetic (1D-HAF) system described by the simple isotropic Hamiltonian $H = -J \sum_i \mathbf{S}_i \cdot \mathbf{S}_{i+1}$, where J is the nearest-neighbor intrachain coupling constant, should depend in a fundamental way on the spin value S . For integer spin values, the 1D-HAF system should exhibit a nonmagnetic *singlet* ground state well separated from the first excited *triplet* state by an energy gap Δ ,¹ whereas the excitation spectrum is expected to be gapless for half-integer-spin values.²⁻⁴ The gap value, estimated to $\Delta \approx 2|J|S \exp(-\pi S)$ from field-theory arguments,^{1,5} is found to decrease rapidly with S and should be sizable only for $S=1$. As a first consequence of the existence of both a singlet ground state and a quantum gap, the 1D-HAF system with integer spin should remain

disordered and should exhibit a finite correlation length ξ at $T=0$. This implies in particular that the equal-time correlation function behaves exponentially, according to the relation^{1,10}

$$\begin{aligned} \langle \mathbf{S}_0 \cdot \mathbf{S}_r \rangle &\approx (-)^r K_0(r/\xi) \\ &\approx (-)^r \left(\frac{r}{\xi} \right)^{1/2} \exp(-r/\xi), \end{aligned} \quad (1)$$

where $K_0(x)$ is the modified Bessel function.

Although a little esoteric in its physical understanding, the "Haldane effect" is now very well supported by many numerical results.⁶⁻¹² In the case of an isotropic system and spins $S=1$, the numerical consensus seems to be realized at values $\Delta \approx 0.411|J|$ and $\xi/d \approx 6$ (d being the interchain distance between adjacent spins). In fact, Δ and ξ are not completely independent quantities but are related through the spin-wave velocity c_0 by the simple relation $\Delta \approx c_0/\xi$, with $c_0 \approx 2.7|J|d$ for the $S=1$ 1D-HAF system.⁹⁻¹²

The first experimental investigations on the Haldane conjecture have been performed on the quasi-1D antiferromagnet CsNiCl_3 ,¹³⁻¹⁷ for which inelastic-neutron-scattering studies in the 1D regime have clearly revealed the existence of an energy gap in the excitation spectrum. This gap has been interpreted within the framework of the Haldane conjecture, slightly modified to incorporate

the non-negligible interchain coupling.¹⁸ Much better candidates are AgVP_2S_6 and $\text{Ni}(\text{C}_2\text{H}_8\text{N}_2)_2\text{NO}_2\text{ClO}_4$ (hereafter abbreviated NENP), for which *no* long-range magnetic ordering could be detected down to the lowest temperatures. The former compound has been extensively studied by inelastic neutron scattering essentially on polycrystalline samples, due to difficulties in growing single crystals of this material.¹⁹ In AgVP_2S_6 , the main experimental results ($\Delta/|J| \approx 0.448$ and $\xi/d \approx 5.5$) are in quantitative agreement with the theoretical predictions for the ideal 1D-HAF system.¹⁹ Unfortunately the large value of the intrachain coupling constant found in this compound ($|J| \approx 58$ meV) limits strongly further investigations like, e.g., inelastic neutron scattering or electron spin resonance studies under field ($\Delta/g\mu_B \approx 200$ T). Finally, NENP appears as the ideal candidate to test experimentally the properties of a Haldane-gap system.

Since the first investigation by Meyer *et al.*²⁰ in 1982 (i.e., before the Haldane's paper) and the pioneering work by Renard *et al.*²¹ in 1986, very comprehensive studies of NENP have been undertaken by various groups, including susceptibility,^{21,22} magnetization,^{23,24} inelastic neutron scattering,^{21,25–28} nuclear magnetic resonance,^{29–31} electron spin resonance,^{32–35} muon spin resonance,³⁶ and specific-heat³⁷ measurements. In all cases, the obtained data have been found to agree remarkably well with the Haldane picture that has been slightly modified to incorporate the orthorhombic anisotropy present in NENP. The observed magnetic properties of NENP can be quantitatively accounted for from the following spin Hamiltonian:

$$H = -J \sum_i \mathbf{S}_i \cdot \mathbf{S}_{i+1} + D \sum_i (S_i^z)^2 + E \sum_i [(S_i^x)^2 - (S_i^y)^2] - \mu_B \mathbf{H} \sum_i \bar{\mathbf{g}} \mathbf{S}_i. \quad (2)$$

In expression (2), D and E are the out-of-plane (OP) and in-plane (IP) anisotropy parameters, respectively, whereas $\bar{\mathbf{g}}$ is the gyromagnetic tensor. Experimental determinations of the parameters of the Hamiltonian (2) give the following values: $J = -(46 \pm 2)$ K, $D/|J| = 0.18 \pm 0.01$, and $E/|J| = 0.02 \pm 0.01$, which show the strong planar anisotropy existing in NENP.

The application of a magnetic field is expected to strongly modify the spin dynamics of an Haldane-gap system. The main effect of a magnetic field is to split the excited triplet in three distinct modes. One of those is expected to soften and finally vanish at a finite characteristic field $H_c \approx \Delta/g\mu_B$.^{38,39} Magnetization measurements in NENP have given clear evidence for the existence of such critical fields.^{23,24} On the theoretical side, the effects of a magnetic field on the spin dynamics have been studied by Affleck³⁸ and Tsvelik³⁹ using bosonic or fermionic field-theory treatments of the anisotropic $S=1$ antiferromagnetic chain. In particular, they have derived analytical expressions for the field dependencies of the three gaps and their respective polarization, which can be directly compared with measurements of the dynamic structure factors $S_{\nu\nu}(\mathbf{q}, \omega)$ associated with the various modes. In the present paper we will describe and discuss

the results of an exhaustive experimental study of magnetic properties of NENP, obtained from inelastic-neutron-scattering measurements in zero field and under magnetic fields applied parallel or perpendicular to the chain axis. Preliminary results have been partly published elsewhere.^{21,25–27} Here we will focus on the field dependencies of the gap values $\Delta_n(H)$ ($n=1,2,3$), correlation lengths $\xi_\nu(H)$ ($\nu=x,y,z$) and polarization factors $P_{\nu\nu}(H)$ of the various modes forming the excited triplet. We will discuss our most significant results in the perspective of recent theoretical developments, both analytical and numerical. Finally we will indicate some perspective and possible continuation to this work.

II. EXPERIMENT

At low temperature, NENP crystallizes in an orthorhombic structure described *approximately* with a space group $Pnma$.²⁰ The lattice parameters at $T=1.5$ K, $a=14.55$ Å, $b=10.25$ Å, and $c=8.27$ Å, have been determined from cold neutron diffraction. The crystallographic structure of NENP consists of long chains of nickel ions running along the b axis, with intrachain spacing $d = \frac{1}{2}b$, in which the Ni^{2+} ions are bridged by strongly covalent NO_2 groups. The chains are well separated from each other by ClO_4 groups, which ensure a very good 1D character of this compound. The single-crystal preparation has been described in previous papers.^{20,21} In the present studies we have used large fully protonated single crystals ($V \approx 1-3$ cm³) of very good quality.

The neutron-scattering experiments have been performed on several thermal neutron three-axis spectrometers (DN1 installed at the reactor Siloe of CEN-Grenoble, IN8 and IN20 installed at the HFR of ILL-Grenoble) and the cold neutron three-axis spectrometer IN12 installed on a cold-neutron guide at ILL. For the thermal-neutron experiments, the neutron incident wave vector was kept fixed at $k_i = 2.662$ Å⁻¹, obtained from vertically focused pyrolytic graphite 002 monochromators. We have used collimators 40'-40'-30' before the sample, analyzer and detector, yielding a typical energy resolution of about 0.6–0.7 meV. For the cold-neutron experiments, the neutron incident wave vector was kept fixed at $k_i = 1.5$ Å⁻¹ and collimations 60'-60'-30' have been used, yielding a improved energy resolution of about 0.13 meV. In both cases appropriate filters (PG graphite or beryllium, respectively) have been used to suppress higher-order contamination. The samples were oriented in all cases with the $(\mathbf{a}^*, \mathbf{b}^*)$ reciprocal plane in the horizontal scattering plane. Figure 1 shows the observable reciprocal space. The 1D antiferromagnetic plane is associated with scattering vectors $\mathbf{Q} = (Q_a, 1, Q_c)$ corresponding to the point $q = \pi$ in the notation generally adopted in theoretical papers. In the rest of this work we have adopted the following convention: $x \equiv c$, $y \equiv a$, and $z \equiv b$. The z axis corresponds to the chain axis, whereas the x axis corresponds to the vertical axis. Consequently, the scattering vectors will be defined by only two components Q_y and Q_z [$\mathbf{Q} = (Q_y, Q_z, 0)$]. In the experiments under field we have used two different types of cryomagnetic

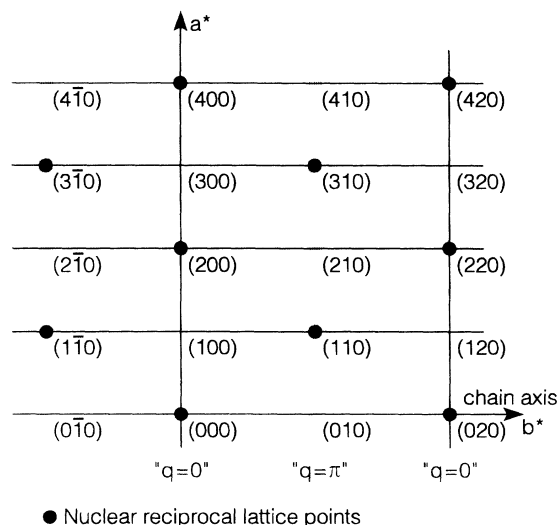


FIG. 1. The (a^*, b^*) plane of the reciprocal lattice. The shaded areas denote the positions of one-dimensional antiferromagnetic planes ($q = \pi$).

equipment. For fields perpendicular to the chain axis, the sample was mounted inside a 10-T *vertical field* cryomagnet, whereas for fields parallel to the chain axis we have used a 5-T *horizontal field* cryomagnet. In the zero-field experiments conventional ILL-type helium-flow cryostats have been used. In all cases, the temperature was controlled between 1.4 and 300 K with a relative accuracy better than 10^{-3} using ILL-type temperature controllers.

III. EXPERIMENTS IN ZERO FIELD

The first evidence for the existence of both a nonmagnetic singlet ground state and an energy gap between the ground state and the first excited state in NENP was obtained by Renard *et al.*²¹ from magnetic susceptibility measurements on single crystals. Whatever field orientation, the susceptibility exhibits a rounded maximum and decreases more or less exponentially as the temperature is lowered below 15 K, as a consequence of the opening of a gap $\Delta \approx 11$ –17 K in the excitation spectrum.²¹ The disappearance of the magnetic fluctuations at low temperature and low energy, a signature of a nonmagnetic ground state, has been unambiguously observed from NMR measurements of the spin-lattice relaxation time T_1 as a function of temperature.^{29–31} Between 50 and 5 K, the fluctuation rate T_1^{-1} has been found to vanish rapidly with T , following an exponential law $T_1^{-1} \propto T \exp(-\Delta/kT)$, with a gap value $\Delta \approx 14$ K consistent with the susceptibility determination.^{21,25} This absence of magnetic fluctuations at low energy has also been confirmed from quasielastic neutron scattering on deuterated samples.²⁸ Neutron-diffraction experiments have unambiguously shown the absence of any long-range magnetic ordering at least down to 0.3 K:^{21,28} no additional superlattice peaks of type $Q = (Q_y, 1, Q_x)$ could be detected in the diffraction patterns at low temperature. This lack of magnetic ordering has been attributed to the very small inter- to intrachain coupling ratio J'/J in

NENP. It is also a direct consequence of the finite value of the correlation length ξ at $T \approx 0$. We will come back more quantitatively to this point later. All these results indicate that the ground state in NENP is a *nonmagnetic singlet ground state* and that *gaps* should be visible in the excitation spectrum.

A. Results at " $q = \pi$ "

A more direct evidence for the existence of such gaps at the antiferromagnetic point has been obtained from inelastic neutron scattering, which is a technique probing directly the various components $S_{nv}(q, \omega)$ of the dynamic structure factor. Following the notations adopted in this paper, the subscript v will label the spin component ($v = x, y, z$), whereas n will characterize the mode number ($n = 1, 2, 3$). Figure 2 shows typical scans in energy measured on the DN1 three-axis spectrometer at two scattering vectors $Q = (0.2, 1, 0)$ (nearly parallel to the chain axis) and $Q = (3.2, 1, 0)$ (which makes a substantial angle with the chain axis). The background has been determined by measuring the inelastic scattering at positions $Q = (0.2, 1.1, 0)$ and $Q = (3.2, 1.15, 0)$, for which the inelastic peaks are expected to be shifted at sufficiently high energy to be outside the explored range. Two gap modes are clearly observed at energies $\Delta_{xy} \approx 1.2$ meV ≈ 14 K and $\Delta_z \approx 2.5$ meV ≈ 29 K. From their dependence of the component Q_y of the scattering vector, we have been able to ascribe unambiguously these two modes to magnetic fluctuations in the xy plane and along the chain axis, respectively. By improving the resolution in energy, we have found that the xy mode split into two distinct

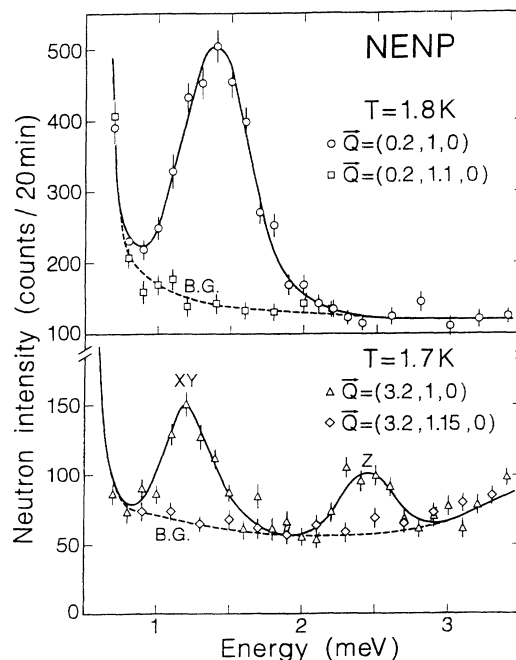


FIG. 2. Constant- Q scans in NENP at different positions in scattering vector [$Q = (0.2, 1, 0)$ (\circ), $(0.2, 1.1, 0)$ (\square) at $T = 1.8$ K; $Q = (3.2, 1, 0)$ (\triangle), $(3.2, 1.15, 0)$ (\diamond) at $T = 1.7$ K]. The lines are the guide to the eye.

modes. Figure 3 shows a typical scan in energy measured on the cold-neutron three-axis spectrometer IN12, at a scattering vector $\mathbf{Q}=(0.3,1,0)$ located nearly along the chain axis. Two gap modes are clearly seen at energies $\Delta_y \approx 1.16$ meV and $\Delta_x \approx 1.34$ meV for a component $Q_y=0.3$. As previously, the polarization of these two modes has been determined by analyzing their dependencies with the scattering vector $\mathbf{Q}=(Q_y,1,0)$. We have found that the low-energy mode 1 contributes mainly to $S_{1y}(q,\omega)$ whereas mode 2 contributes mainly to $S_{2x}(q,\omega)$.

Thus, three gaps are unambiguously observed in NENP, which demonstrate the *triplet nature* of the excited state. This is again in agreement with the theoretical predictions for a Haldane-gap system. From our data, it appears that each gap mode is associated with only one type of fluctuation, without polarization mixing in zero field. The experimental data at low temperatures and not too small energies (i.e., $\hbar\omega/kT \gg 1$), have been analyzed using the following Lorentzian expression (in the most general anisotropic case):

$$S_{nv}(q,\omega) \approx S_{n0} \frac{P_{nv}}{\kappa_{nv} \Gamma_n} \frac{1}{1 + [(q - k_{AF})/\kappa_{nv}]^2 + \{[\omega - \omega_n(q)]/\Gamma_n\}^2} \quad (3)$$

in which $k_{AF}=2\pi/b$ is the 1D AF wave vector, $\omega_n(q)$ is the energy of mode n ($n=1,2,3$) at wave vector q , κ_{nv} are coefficients characterizing the scale in q associated with the various components v ($v=x,y,z$), P_{nv} are the polarization factors and Γ_n is the fluctuation rate associated with the n th mode. In Eq. (3), the normalization factor S_{n0} contains the statistics of the elementary excitations. Therefore, it is also expected to be temperature dependent. It is important to note that relation (3) is a generalization to the anisotropic case of a theoretical expression

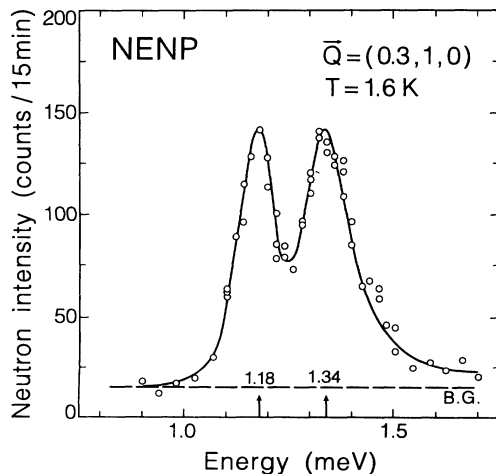


FIG. 3. High-resolution constant- Q scan for NENP at $T=1.6$ K and $\mathbf{Q}=(0.3,1,0)$ showing the splitting of the xy mode. The solid line is a guide for the eye.

established for the isotropic case.⁴¹ To our knowledge, this generalization has never been precisely demonstrated. From general arguments,⁴¹ the fluctuation rate Γ_n is expected to depend exponentially on T , following the relation $\Gamma_n \approx \Gamma_{n0} \exp(-\Delta_n/kT)$, where the prefactor Γ_{n0} can depend slightly on H and T . At sufficiently small temperatures such that $kT \ll \Delta_n$, $S_{nv}(q,\omega)$ can be rewritten according to the simpler expression

$$S_{nv}(q,\omega) \approx S_{n0} \frac{P_{nv}}{\kappa_{nv}} \frac{1}{\sqrt{1 + [(q - k_{AF})/\kappa_{nv}]^2}} \delta[\omega - \omega_n(q)] \quad (3')$$

In the vicinity of the antiferromagnetic point k_{AF} , we have used the following quadratic approximation for the magnon dispersion relations:⁵

$$\omega_n(q) \approx \sqrt{(\Delta_n)^2 + c_0^2(q - k_{AF})^2}, \quad (4)$$

where c_0 is the spin-wave velocity previously defined, considered here as an adjustable parameter. In zero field, these notations can be simplified, because each mode is associated with a single polarization (this is no more the case under field). In the following we will rename the three gaps at $H=0$ as Δ_v ($v=x,y,z$) and the corresponding correlation lengths as $\xi_v = \kappa_v^{-1}$. Our experimental data at low temperature have been found in good agreement with δ functions in energy as given by relation (3'). This is well illustrated by the observation of resolution-limited widths in energy, which imply long lifetimes for the corresponding excitations. A more quantitative analysis would require to properly introduce the instrumental resolution function $R(q,\omega)$. Such an analysis could certainly explain the slightly asymmetric line shape observed experimentally as resulting from the folding of the physical function $S_{nv}(q,\omega)$ with the resolution function. However, this procedure has not been done here. We think it is better to consider the neutron intensity integrated in energy, defined by the expression $S_v(q) = \int S_v(q,\omega) d\omega$. The integration over ω cancels the effect of the resolution in energy and, in principle, one has only to take into account for the q resolution, characterized by a full width at half maximum (FWHM) in the range $\Delta q^{\text{res}} \approx 0.010-0.015$ r.l.u., depending on the k_i used. The fact that $\Delta q^{\text{res}}/2 \ll \kappa \approx 0.05$ r.l.u. makes these corrections completely negligible. From relation (3'), one obtains immediately the following square-root Lorentzian expression for $S_v(q)$:

$$S_v(q) \propto \frac{\xi_v}{\sqrt{1 + (q - k_{AF})^2 \xi_v^2}} \quad (5)$$

This expression can be obtained directly by Fourier transforming the correlation function given by Eq. (1). It shows that at $q = k_{AF}$, the static structure factor $S_v(k_{AF})$ is directly related to the correlation length ξ_v . Assuming that the relation $\Delta_v \approx c_0 \cdot \xi_v^{-1}$ is valid for an anisotropic system leads to the simple relation $S_v(k_{AF}) \propto \Delta_v^{-1}$, which can be checked experimentally. The correlation lengths

ξ_v can be derived in a more direct manner from the FWHM Δq associated with $S_v(q)$, using the relation $\xi_v = 2\sqrt{3}/\Delta q$. Consequently, neutron-scattering measurements of $S_v(q)$ should allow an accurate determination of these fundamental parameters.

From the energy scan at $Q=(3.2,1,0)$ previously described (see Fig. 2) and after correction by the usual geometrical factors depending on Q and k_f (the final neutron wave vector), we have deduced the following experimental values (in arbitrary units) for the components S_x and S_z :

$$S_x(k_{AF}) = 100 \pm 10$$

and

$$S_z(k_{AF}) = 50 \pm 10 \approx S_x(k_{AF}) \cdot \frac{\Delta_x}{\Delta_z},$$

whereas the third component $S_y(k_{AF})$ was almost suppressed by the geometrical factor $1-(Q_y/Q)^2$ and hence not accessible from this measurement. Our experimental data confirm quantitatively the relation $S_v(k_{AF}) \propto \Delta_v^{-1}$. This indicates that the relation $\Delta_v \propto \xi_v^{-1}$ is valid in NENP, at least in what concerns the xy and z components. The same procedure applied to the x and y modes leads to a somewhat different conclusion: experimentally (see, for example, Fig. 3), the energy-integrated intensities at $q = k_{AF}$ of the magnetic fluctuations along the x and y directions are *not simply proportional* to Δ_x^{-1} and Δ_y^{-1} . In fact, using various samples, cryostats or spectrometers, we have *systematically* found $S_x(k_{AF})$ *slightly larger* than $S_y(k_{AF})$, despite relatively large error bars: $S_x(k_{AF}) = 100 \pm 10$ (after normalization), whereas $S_y(k_{AF}) = 90 \pm 10$. The relation $S_y(k_{AF}) \propto \Delta_y^{-1}$, if correct, would lead to an estimate $S_y(k_{AF}) \approx 115$, a value largely outside the experimental accuracy. A possible explanation from Eq. (5) would be to suppose that the correlation length ξ_x is about 10% larger than the correlation length ξ_y (assuming polarization factors $P_{1y} \approx 1$ and $P_{2x} \approx 1$). Thus, the analysis of integrated intensities at $q \approx k_{AF}$ has revealed the existence of anisotropic correlation lengths, with values of ξ_x , ξ_y , and ξ_z in the ratios 1.05, 0.95, and 0.5, respectively. Qualitatively this anisotropic character should reflect the orthorhombicity existing in NENP. However, we have no quantitative explanation for these numbers, nor for the unusual role played by the in-plane anisotropy term. In what follows, it will be useful to introduce the in-plane correlation length in absence of in-plane anisotropy defined by $\xi_{xy} \approx (\xi_x + \xi_y)/2$. We will come back later on the experimental determination of this important quantity.

From our experimental data, a weak dispersion of modes 1 and 2 has been observed along the a^* axis (perpendicular to the chain axis). This dispersion is found to be very similar for both modes, as shown in Fig. 4. Both dispersion curves appear shifted one from the other by about 0.18 ± 0.01 meV $\approx 2 \pm 0.1$ K. The minima are found for odd q_a values at energies $\Delta_y^0 \approx 1.05$ meV and $\Delta_x^0 \approx 1.23$ meV, whereas the maxima are seen for even q_a values, at energies 1.23 and 1.41 meV, respectively. Such

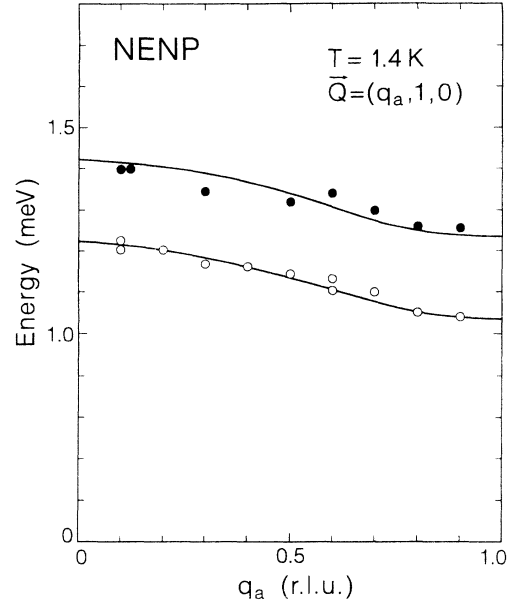


FIG. 4. Dispersion of the magnetic excitations in NENP at 1.4 K. The open and solid circles show the experimental dispersion for the two modes in the a^* direction perpendicular to the chain axis. The solid line curves are best fits to Eq. (6).

a periodicity is characteristic of an antiferromagnetic interchain coupling. The dispersion relation along the c^* axis (also perpendicular to the chain axis) has not been measured for evident geometrical reasons. Therefore, it is not certain that the wave vector $\mathbf{k}=(1,1,0)$ corresponds to the minimum in energy of the excitation spectrum. We have analyzed our experimental data using the following dispersion relations, which can be easily derived within the framework of classical spin-wave theory:

$$\Delta_v(q_a) \approx \sqrt{(\Delta_v^0)^2 + (\Delta E)^2 [(1 + \cos \pi q_a)/2]^2} \quad (6)$$

in which q_a is expressed in units $2\pi/a$ and where ΔE characterizes the amplitude of the dispersion. In deriving relation (6), we have implicitly taken into account that there is two chains per unit cell along the a axis. The solid lines in Fig. 4 represent the best fits to the relation (6) with a parameter $\Delta E \approx 0.65 \pm 0.05$ meV. This dispersion is due to the weak interchain coupling J' . But the precise relation between ΔE and J' is unknown for NENP. Nevertheless, an estimate of the ratio J'/J can be obtained from the classical spin-wave result $\Delta E \approx 2S\sqrt{zz'}|JJ'|$, where z is the number of adjacent spins in a chain ($z=2$) and z' the number of adjacent chains. For simplicity we have assumed the existence of only one kind of interchain coupling in NENP ($z'=4$), an approximation in contradiction with the orthorhombic character of the crystallographic structure. From the experimental data one gets a ratio $|J'/J| \approx 8 \times 10^{-4}$ (or equivalently $|z'J'/zJ| \approx 1.6 \times 10^{-3}$). This ratio, slightly larger than the one determined in Ref. 21, is more than 1 order of magnitude smaller than the critical ratio $|J'/J|_c \approx 0.4/z'(\Delta/J)^2$, below which quantum fluctuations are expected to be sufficiently strong to prevent any

long-range ordering, even at $T=0$.^{9,42,43} Applied to the case of NENP, the above relation gives a critical value $|J'/J|_c \approx 0.016$, much larger than the experimental determination of $|J'/J|$.

As previously mentioned, the splitting of the excited triplet is well understood as an effect of the finite orthorhombic single-ion anisotropy existing in NENP. The average value $\Delta_0 = (\bar{\Delta}_x + \bar{\Delta}_y + \bar{\Delta}_z)/3$, where the quantities $\bar{\Delta}_\nu$ ($\nu=x,y,z$) are obtained by averaging the gap values along the direction perpendicular to the chain, should not contain to first order the effects of anisotropy or inter-chain coupling. Therefore, this quantity is expected to be a reasonable estimate of the gap value for the ideal $S=1$ 1D-HAF system. For NENP one obtains $\Delta_0 \approx 1.7$ meV ≈ 20 K, which implies a dimensionless ratio $\Delta_0/|J| = 0.42 \pm 0.02$ (using $|J| \approx 4$ meV ≈ 46 K) in good quantitative agreement with the best numerical determinations. This is one of the best proofs for the applicability of the Haldane-gap theory in NENP. By defining the xy gap in absence of in-plane anisotropy (i.e., assuming $E \approx 0$) by the relation

$$\bar{\Delta}_{xy} = (\bar{\Delta}_x + \bar{\Delta}_y)/2 \approx 1.23 \text{ meV} \approx 14.3 \text{ K},$$

we deduce for the splitting resulting from the out-of-plane (OP) anisotropy term a value $\bar{\Delta}_z - \bar{\Delta}_{xy} \approx 1.25$ meV ≈ 14.5 K. This value agrees quantitatively with the numerical determination^{9,11} $\Delta_z - \Delta_{xy} \approx 1.8 - 1.9D$, if we assume an anisotropy parameter in the range 7.6–8 K, implying a ratio $D/|J| \approx 0.17$. This ratio is slightly smaller than the one extracted from the analysis of susceptibility measurements,^{23,44} which was in the range 0.19–0.20. A possible explanation for this discrepancy of about 10% may result from a temperature dependence of the OP anisotropy parameter D arising from a small change in the geometry of ethylenediamine molecules. Recently, Golinski *et al.*⁴⁰ have determined from numerical calculations on finite-size systems the effect of an in-plane anisotropy term, assuming a realistic ratio $D/|J| \approx 0.18$. They have derived the linear relation $\Delta_x - \Delta_y \approx 4E$ for the splitting of the xy mode, which leads to the estimate $E/|J| \approx 0.012$, using the experimental result $\Delta_x - \Delta_y \approx 0.18$ meV. This value is consistent with previous determinations of E from susceptibility and ESR measurements.^{21,25,32}

B. Wave-vector dependency of gaps

The wave-vector dependency of the magnetic excitations is very important to determine for a Haldane-gap system. Two features can be considered as supplementary signatures of the Haldane ground state: the finite correlation lengths at $T \approx 0$ and the 2π periodicity of the excitation spectrum. The latter implies in particular completely different behavior at $q=0$ and $q=k_{AF}$.^{11,12,45–47}

Due to the absence of quasielastic scattering at low temperature, the dynamic correlation lengths ξ_ν ($\nu=x,y,z$) can be estimated from the wave-vector dependency around $q \approx k_{AF}$ of the intensity integrated in energy over the inelastic peak. In principle, this last quantity

is directly related to the static spin-correlation function $S_\nu(q)$, which is nothing else than the Fourier transform of the spin-spin correlator $\langle S_0^\nu \cdot S_r^\nu \rangle$. However, such determinations have been more or less difficult to undertake, depending on the spin-component considered. In particular, due to the very weak intensity resulting from the necessity to measure at large Q_y components, it has not been possible to obtain sufficiently accurate data for the component $S_z(q)$. Only the dispersion relation has been measured in that case, in a relatively small range of q values. In contrast, accurate data could be obtained for the in-plane fluctuations contributing to $S_{xy}(q)$. Figure 5 displays scans in energy performed at several scattering vectors $\mathbf{Q} = (0.2, 1+q_b, 0)$, with q_b values up to about $0.1k_{AF}$. Both a shift in the peak position and a decrease in the intensity are observed. Similar results, although with less accuracy, have been obtained for the out-of-plane component. Figure 6 shows the dispersion relation for the xy and z modes, taken as the energy of the intensity maximum. The experimental data have been analyzed using the theoretical dispersion relations given by Eq. (4). The best fitting is achieved with a spin-wave velocity $c_0 \approx 30$ meV/r.l.u. ≈ 50 meV \AA . Using the appropriate exchange coupling constant $|J| \approx 4$ meV, one obtains a dimensionless ratio $c_0/|J|d \approx 2.5$, which is only 8% smaller than the theoretical prediction.^{9–12} Unfortunately, due essentially to a contamination by incoherent libration modes arising from the *protonated* ethylenediamine molecules, it has not been possible from the present experiments to determine unambiguously the magnon dispersion relation at larger $|q - k_{AF}|$ values.²⁷ This determination has been successfully undertaken by Ma *et al.*²⁸ down to $q \approx 0.3k_{AF}$, using a large *deuterated* sample. Their experimental results are found quite consistent not only with our own experimental results (very similar in the vicinity of the antiferromagnetic point) but also with theoretical results obtained from numerical calculations,^{10–12} in particular, for the dispersion and the inten-

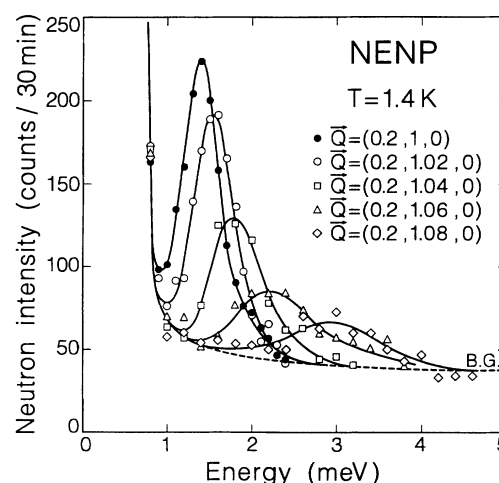


FIG. 5. Typical energy scans in NENP at $T=1.4$ K as a function of the reduced wave vector q_b , showing the dispersion of the magnetic excitations along the chain. The lines are guides to the eye.

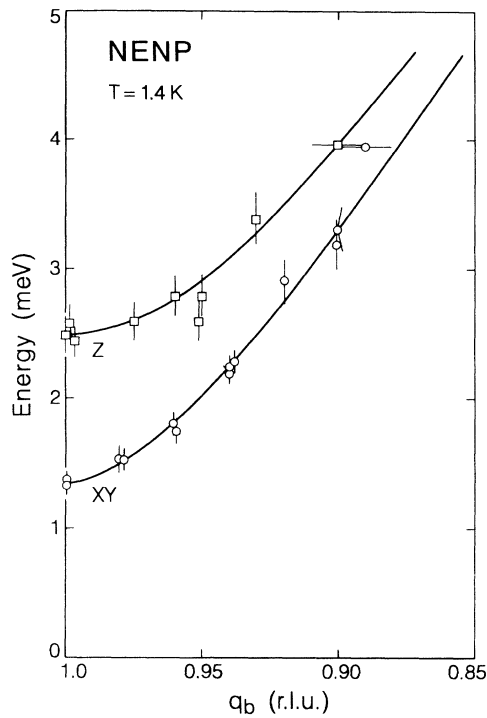


FIG. 6. Dispersion of the magnetic excitations in NENP at 1.4 K in the b^* direction parallel to the chain axis. The open symbols are the experimental points. The solid lines correspond to the theoretical prediction given by Eq. (4).

sity of modes. The most interesting feature is the slight asymmetry in the excitation spectrum observed on both sides of $k_{AF}/2$, which has been interpreted as a signature of the 2π periodicity reflecting the absence of broken translational symmetry in the ground state of NENP.

Below $0.3k_{AF}$, the nature of the magnetic excitations is expected to change drastically. The theory for the ideal system^{11,12,45,47} predicts the existence of a continuum of two-magnon excitations which should display at $q=0$ an energy gap twice that at $q=k_{AF}$. Anisotropy terms are expected to modify only slightly this picture.^{11,47} In the real case of NENP gap modes at $2\Delta_{xy} \approx 2.4$ meV (OP fluctuations) and $\Delta_{xy} + \Delta_z \approx 3.7$ meV (IP fluctuations) have been predicted, although with very weak intensities.⁴⁷ We have performed a series of inelastic-neutron-scattering experiments at small q values [in the range $(0-0.2)k_{AF}$] in order to try to detect these very unusual features. Our experimental data, obtained from scans in energy between -2 and 6 meV performed at two equivalent scattering vectors $\mathbf{Q}=(1.2, 2-q, 0)$ (probing the xy fluctuations) and $\mathbf{Q}=(3.2, -q, 0)$ (probing the xz fluctuations), have revealed the *absence of any sizable magnetic signal* in the vicinity of $q \approx 0$, despite counting times as long as 4 h per point. Only upper limits for the various structure factors have been deduced from these very difficult experiments, implying that

$$S_v(q \leq 0.2k_{AF}) \ll S_{xy}(q \approx k_{AF})/30.$$

Up to now, there is *no* clear experimental evidence nei-

ther for the existence of a continuum nor for a doubling of the gap at $q=0$. Our negative results are consistent with very small structure factors, predicted theoretically⁴⁷ to be controlled by the factors $(E/J)^2$ and $(D/J)^2$. Numerical calculations on finite-size systems¹⁰⁻¹² have given more precise estimates for the static structure factors, which below $0.2k_{AF}$ are 2 orders of magnitude smaller than those determined at the antiferromagnetic point. These very small intensities will certainly prevent further investigations by neutron scattering, even using fully deuterated samples. The same conclusion was obtained in Ref. 28.

The energy-integrated intensity of the in-plane fluctuation near k_{AF} is shown in Fig. 7 as a function of q along the chain. Although it appears very difficult from our data to distinguish between a simple Lorentzian and the square-root Lorentzian function given by Eq. (5), our experimental results suggest in both cases a *finite* value for the dynamical correlation length ξ_{xy} associated with xy fluctuations. The best fitting to the theoretical relation (5) gives a reduced value $\xi_{xy}/d \approx 8$, which is about 30% larger than the theoretical prediction for the ideal 1D-HAF system. This small discrepancy can be understood if we assume that the relation $\xi_{xy} \approx c_0 \Delta_{xy}^{-1}$ is valid for the IP components. However, we have seen in the previous section that such a relation was not quantitatively confirmed for ξ_x and ξ_y alone, showing the unusual role played by an Ising-like anisotropy term. As already mentioned, it has not been possible to determine *directly* an accurate value for the correlation length ξ_z . Nevertheless, from the expected relation $\xi_z \approx c_0 \Delta_z^{-1}$, one can estimate $\xi_z/d \approx 4$. A further very interesting experimental

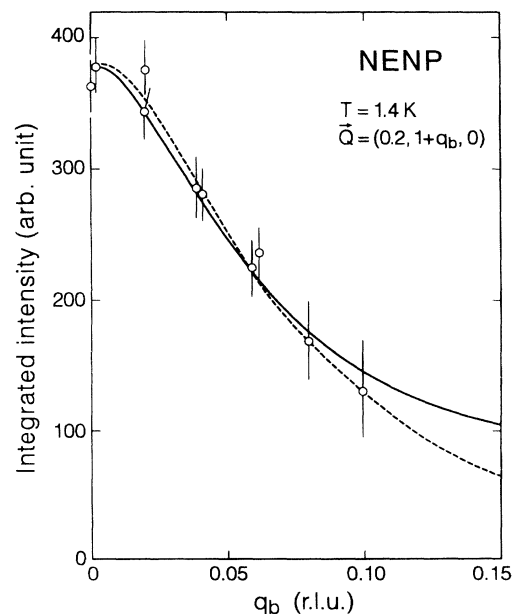


FIG. 7. Intensities integrated in energy of the xy mode as a function of the reduced wave-vector component q_b parallel to the chain axis. The solid line corresponds to the square-root Lorentzian function given by Eq. (5). The dashed line is a fit to a simple Lorentzian function.

problem would be to determine separately ξ_x and ξ_y . We believe that polarized neutron-scattering experiments would allow to verify that ξ_x is indeed larger than ξ_y , as suggested by the present results in zero field.

IV. FIELD DEPENDENCIES OF GAPS AND POLARIZATION

As previously mentioned, the application of a magnetic field in a Haldane-gap system is expected to suppress the many body quantum effect at the origin of the Haldane ground state. The excited triplet is split by the Zeeman effect into three distinct modes. One of these modes is expected to vanish at a critical field H_c , which is more or less directly related to the gap value Δ (typically one expects $H_c \approx \Delta/g\mu_B$). Magnetization measurements on single crystals have given clear evidence for the existence of such critical fields in NENP.^{23,24} The most interesting feature that has emerged from these measurements is certainly the anisotropic character of H_c observed in a field applied along the chain ($H_c^z \approx 92-98$ kOe) or perpendicular to the chain ($H_c^{xy} \approx 125-140$ kOe). As shown by several authors,^{24,38,39} this anisotropic behavior reflects both the orthorhombic single-ion anisotropy and the existence of unconventional field dependencies of the gaps $\Delta_n(H)$. Experimental determinations of field dependencies of the gaps in NENP have been tentatively undertaken from various macroscopic (e.g. magnetization^{23,24} or specific-heat³⁷ measurements) as well as microscopic techniques [e.g. INS (Refs. 26 and 27) or NMR (Refs. 29–31)]. Usually, the analysis of experimental data requires a “good” model and in most cases the procedure consists in verifying that there are no strong inconsistencies between the experimental data and the model. For instance, the analysis of NMR data requires a precise knowledge of the line shape at very low energy (in fact for $\omega/T \ll 1$), certainly not described by Eq. (3). In contrast, inelastic neutron scattering allows a much more direct determination of the field dependencies of the gaps, relatively independent of any model. The main problem is to determine completely the various components $S_{nv}(q, \omega, H)$ of the dynamic structure factor. We will be particularly interested in the determination of the field dependencies of some relevant quantities like, e.g., the gap values $\Delta_n(H)$ or the various components of energy-integrated structure factors $S_{nv}(k_{AF}, H)$ measured at the antiferromagnetic point. These are in fact the most important quantities needed for a fruitful comparison with the theoretical models, together with the various correlation lengths $\xi_v(H)$.

A. Results in field parallel to the chain axis

In this configuration we have used a 5-T horizontal field cryomagnet, which reduces the neutron beam access to only 20° in the equatorial plane. For evident geometrical reasons, it has only been possible to study the in-plane modes at the scattering vector $Q = (0.3, 1, 0)$ located nearly along the chain axis. In Fig. 8, we show typical scans in energy measured at a temperature $T \approx 1.6$ K for three values of the field, $H = 0, 20$, and 40 kOe. Changes are

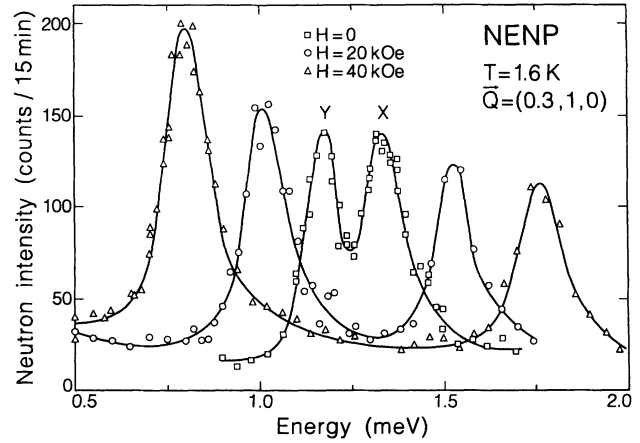


FIG. 8. Constant- Q scans at $Q = (0.3, 1, 0)$ and $T = 1.6$ K for three values of the magnetic field applied along the chain axis; $H = 0$ (\square), $H = 20$ kOe (\circ), and $H = 40$ kOe (\triangle). The solid lines are guides to the eye.

observed for both modes, not only in the peak position but also in intensity. Figure 9 shows the field dependencies of the gaps Δ_1 and Δ_2 , deduced from these experimental data after correction for the usual neutron factor $k_f^3 \cot \theta_A$ (where θ_A is the Bragg angle of the analyzer). Mode 1 (mainly y polarized in zero field) softens when the field is increased, the energy being reduced from 1.16 meV at $H = 0$ to 0.81 meV at $H \approx 40$ kOe. In contrast, mode 2 (mainly x polarized in zero field) increases continuously, from 1.34 meV at zero field to 1.76 meV at the maximum field. As already said, it has not been possible to follow the third mode. However, this mode should

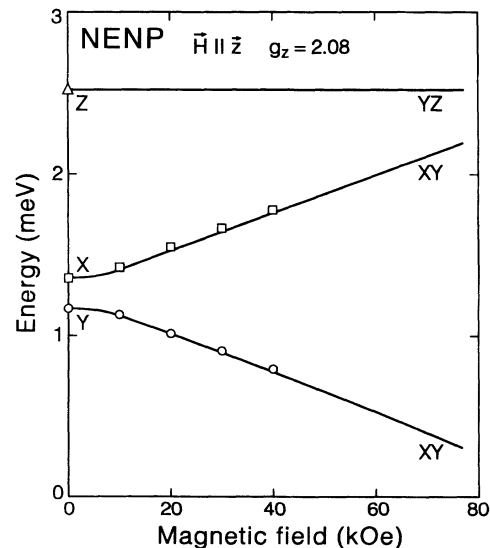


FIG. 9. Field dependence of the gaps at $q = \pi$ and $T = 1.6$ K, in a field parallel to the chain. The open symbols (\circ and \square) are the experimental points associated to modes 1 and 2. Mode 3 has been measured only in zero field. The solid lines correspond to the fermionic field-theory predictions given by Eq. (7).

remain constant under field^{38–40} from general arguments. In Fig. 9, the solid lines represent theoretical curves resulting from the fermionic field-theory treatment of the Hamiltonian (2), calculated from the following relations:^{38,40}

$$\Delta_{1,2}(H_z) = \frac{\Delta_x + \Delta_y}{2} \pm \sqrt{[(\Delta_x - \Delta_y)/2]^2 + (g_z \mu_B H_z)^2}, \quad (7)$$

$$\Delta_3(H_z) = \Delta_z,$$

where the g_v are the components of the anisotropic gyromagnetic tensor. As noted by Golinelli *et al.*,⁴⁰ these expressions are formally identical to those derived from a simple perturbative treatment of the Zeeman term, in the presence of orthorhombic anisotropy. Clearly, the experimental behavior is quantitatively accounted for by relation (7), taking a parameter $g_z \approx 2.08$ slightly smaller than the one determined from susceptibility measurements, which gave $g_z \approx 2.18$.^{21,25} We have attributed this difference of about 5% to the probable existence of temperature effects similar to those responsible for the decrease of D [recall that $D \propto (g_{xy} - g_z)$]. The critical field H_c^z , defined as being the field at which the Δ_1 gap vanishes, is given by the simple expression:

$$H_c^z = \frac{\sqrt{\Delta_x \Delta_y}}{g_z \mu_B} \approx \frac{\Delta_{xy}}{g_z \mu_B}, \quad (8)$$

where we have introduced the gap value in absence of in-plane anisotropy: $\Delta_{xy} = (\Delta_x + \Delta_y)/2$. From the experimental determination $\Delta_{xy} \approx 1.23$ meV one calculates $H_c^z \approx 100$ kOe, a value in good agreement with the high-field magnetization measurements.^{23,24} This confirms unambiguously that, in the case of a field parallel to the chain axis, the critical field is mainly controlled by the xy gap and not at all by the z gap, as classically expected.

As previously, our experimental data have been analyzed by considering the energy-integrated intensities. Figure 10 shows the experimental results for modes 1 and 2. The experimental data plotted in this figure have been corrected by the usual geometrical factors depending on Q and k_f , and finally normalized to the previous data in zero field. For the reasons mentioned above, it has not been possible to determine univocally and independently the different polarization for these two modes, which both should be strongly xy polarized from symmetry arguments. Theoretically, one expects isotropic polarization factors (with $P_{nx} \approx P_{ny} \approx \frac{1}{2}$) for fields sufficiently strong, this resulting from the nearly perfect axial symmetry induced by the field.^{38,40} Unfortunately, the analysis of our experimental data has been complicated by the lack of precise expressions for the structure factor components $S_{nx}(H)$ and $S_{ny}(H)$. Experimentally, due to the scattering vector Q chosen, we have measured the total quantities $S_n(H) \approx S_{nx}(H) + S_{ny}(H)$, taking into account the fact that $1 - (Q_y/Q)^2 \approx 1$. The intensities $S_n(H)$ ($n=1,2$) are both found to increase in increasing field, the intensity of mode 1 increasing apparently more rapidly than the intensity of mode 2 (see Fig. 10). This result confirms our previous conclusions that $S_{nv}(k_{AF}, H)$ is not simply related to $\Delta_n^{-1}(H)$ for all modes. Surely, the

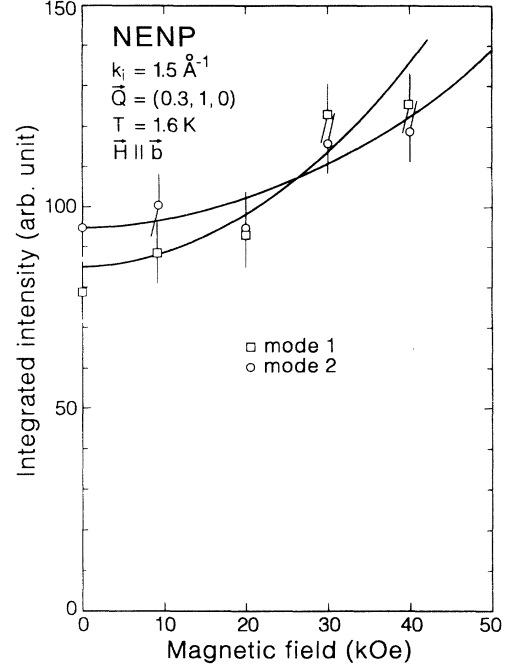


FIG. 10. Field dependence of the intensity integrated in energy at $q = \pi$ for modes 1 and 2. The solid lines are fitted to expressions quadratic in H as explained in the text.

polarization factors $P_{nv}(H)$ and the correlation lengths $\xi_v(H)$ should play an important role. From Eq. (5) one predicts $S_{nv}(k_{AF}, H) \propto P_{nv}(H)/\kappa_{nv}(H)$. Such relations have been tentatively applied to the analysis of our experimental data. Neglecting in a first approximation the in-plane anisotropy (i.e., assuming $\kappa_{nx} \approx \kappa_{ny} \approx \kappa_n$) and taking into account the fact that $P_{nx} + P_{ny} \approx 1$ for each mode, we deduce the simple relation: $S_n(k_{AF}, H) \propto \kappa_n^{-1}(H)$. The various coefficients $\kappa_n^{-1}(H) \equiv \xi_n(H)$ can be viewed as pseudocorrelation lengths, related to the real correlation lengths ξ_x and ξ_y by $\xi_1 + \xi_2 \approx \xi_x + \xi_y \approx 2\xi_{xy}$. This last relation can be easily obtained by applying the sum rules for the correlation lengths,^{48,54} assuming that mode 3 is only z polarized (in our case this gives $\xi_x \propto [S_{1x}(k_{AF}) + S_{2x}(k_{AF})]$ and $\xi_y \propto [S_{1y}(k_{AF}) + S_{2y}(k_{AF})]$) and by taking into account the approximate xy symmetry. Our experimental results can be understood by assuming an increase of both ξ_1 and ξ_2 , which also implies an increase of ξ_{xy} . Such a behavior for the in-plane correlation length has been predicted theoretically to occur in the vicinity of the critical field.^{49,50} At low field we have analyzed our experimental data from relations quadratic in field. The solid lines in Fig. 10 correspond to the best fitting of the energy-integrated intensities to the expression

$$S_n(k_{AF}, H) \approx S_n(0) \cdot \left[1 + A_n \left(\frac{H}{H_c^z} \right)^2 \right]$$

with parameters $S_1(0) \approx 85$, $S_2(0) \approx 95$, $A_1 \approx 3.8$, and $A_2 \approx 1.9 \approx A_1/2$. Neglecting the small in-plane anisotropy, we deduce for the field dependency of the in-plane

correlation length ξ_{xy} the quadratic relation:

$$\xi_{xy}(H) \approx \xi_{xy}(0) \cdot \left[1 + A_{xy} \left(\frac{H}{H_c^z} \right)^2 \right]$$

with $\xi_{xy}(0)/d \approx 8$ (previously determined) and a rather large coefficient $A_{xy} \approx (A_1 + A_2)/2 \approx 2.8$. It is difficult to further discuss the physical meaning of the parameter A_{xy} , due to the lack of precise theories. An interesting result is the relatively fast increase of the correlation length in a field parallel to the chain axis, even well below H_c^z . We believe that this behavior is due to the xy symmetry and to the strong quantum character of the system. As previously mentioned, the correlation length $\xi_z(H)$ has not been measured in the present experiment. Nevertheless, from very general arguments,^{49,50} this component is expected to be nearly field independent up to the critical field H_c^z .

B. Results in field perpendicular to the chain axis

In the configuration for which the field is applied along the x axis, we have used a 10-T vertical field cryomagnet, allowing observations in the equatorial plane over an angular range of nearly 110° . This situation turns out to be much more favorable, because it becomes possible to study all the three modes and their respective polarization, by changing the scattering vector component Q_y . It is also possible to study the dispersion of the magnetic excitations under field in the vicinity of k_{AF} . The high-energy mode 3 has been studied on various thermal neutron three-axis spectrometers: DN1 (Siloe), IN8, and IN20 (ILL), whereas modes 1 and 2 have been studied on the cold-neutron three-axis spectrometer IN12 (ILL). In order to allow quantitative comparisons, the various sets of measurements have been normalized first on the intensity of mode 2 (which has been systematically measured at high field) and secondly to the previous data in zero field. Figure 11 displays typical scans in energy realized

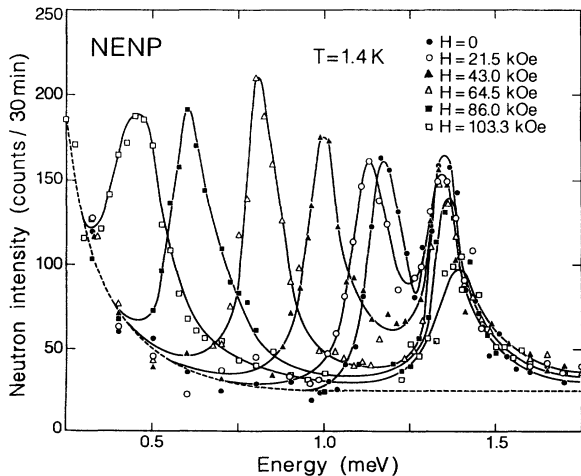


FIG. 11. Constant- Q scans at $Q=(0.3,1,0)$ and $T=1.4$ K for several values of the magnetic field applied along the c^* axis perpendicular to the chain axis. The solid and dashed lines are guides to the eye.

at a scattering vector $Q=(0.3,1,0)$ for a temperature $T=1.4$ K and magnetic fields up to 103 kOe. Mode 1 softens with increasing field, in analogy to the results obtained with the field parallel to the chain axis. The energy is reduced from 1.16 meV in zero field to 0.47 meV for $H=103$ kOe. In contrast to the previous field configuration, mode 2 is found to be only weakly field dependent, increasing slightly from 1.34 meV in zero field to 1.40 meV at maximum field. The energy of mode 3 increases continuously from 2.5 to 3.3 meV in the same field range. This variation with field is well illustrated in Fig. 12, which shows results of an energy scan at the scattering vector $Q=(-0.5,1,0)$ in a field $H \approx 96$ kOe. A two-peak structure is observed, originating mainly from xy fluctuations. Whereas the first peak was attributed unambiguously to mode 2, the second peak at 3.3 meV has been attributed to mode 3, which now presents a *mixed* polarization ($z+xy$). By changing the Q_y component, it was shown that mode 3 was mainly yz polarized. We will come back to the quantitative analysis of this contribution later. Figure 13 shows the experimental field dependency of the three gaps Δ_n . On this figure, the solid lines result from a calculation based on the fermionic field-theory treatment³⁹ generalized by Affleck in order to take into account the in-plane anisotropy term.³⁸ The obtained expressions can be rewritten in a simpler manner according to the following expressions:⁴⁰

$$\Delta_{1,3}(H_x) = \frac{\Delta_z + \Delta_y}{2} \pm \left[\left(\frac{\Delta_z - \Delta_y}{2} \right)^2 + (g_x \mu_B H_x)^2 \right]^{1/2}, \quad (9)$$

$$\Delta_2(H_x) = \Delta_x,$$

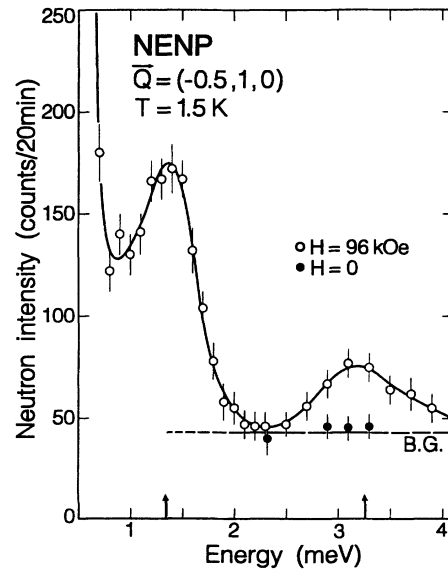


FIG. 12. Constant- Q scan at $Q=(-0.5,1,0)$ and $T=1.5$ K for a magnetic field perpendicular to the chain axis. Open circles are the experimental points for $H=96$ kOe. Solid circles have been obtained at $H=0$. The solid line is a guide to the eye.

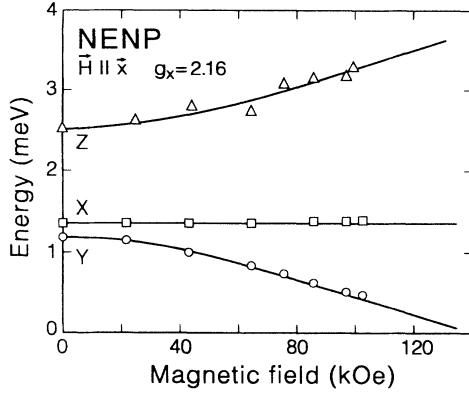


FIG. 13. Field dependence of the gap energies at $q = \pi$ and $T = 1.4$ K in a field perpendicular to the chain axis. The solid lines correspond to the fermionic field-theory predictions given by Eq. (9).

which are valid only at the antiferromagnetic point ($q \approx k_{AF}$). Quite similar to the previous field configuration, expressions (9) can be derived more simply from a perturbation treatment of the Hamiltonian (2). Again, the experimental behavior is quantitatively accounted for by the theory, except the weak change (by 5%) in Δ_z . In the fitting procedure we have obtained a value $g_x \approx 2.16$, which is 3% smaller than the value extracted from susceptibility measurements.^{21,25} The critical field H_c^x at which the gap Δ_1 vanishes, is given by the relation

$$H_c^x = \frac{\sqrt{\Delta_z \Delta_y}}{g_x \mu_B}. \quad (10)$$

Now, the critical field H_c^x depends on both Δ_z and Δ_y . From the experimental values $\Delta_y \approx 1.16$ meV, $\Delta_z \approx 2.5$ meV, and $g_x \approx 2.16$, we estimate a critical field $H_c^x \approx 136$ kOe. This value is slightly larger than the one determined from high-field magnetization measurements.^{23,24} A better agreement would require to correct Δ_y and Δ_z for the small interchain dispersions along the a and c axes or to introduce the small interchain couplings J'_a and J'_c in the theory. Be that as it may, at this stage of our analysis it appears that the comparison between experimental data and theory strongly support the fermionic field-theory approach, at least in the range of field values used in the present experiments. A similar conclusion has emerged from an analysis of macroscopic measurements like, e.g., susceptibility or specific-heat measurements.⁵¹ Our experimental results are in perfect agreement with recent numerical calculations on finite size systems in applied field by Golinelli *et al.*⁴⁰ Finally, they are found to be quite consistent with the ESR measurements,³²⁻³⁴ which in fact have probed nothing else but the transitions between the various excited modes at $q = k_{AF}$.^{33,38} Our determination of components of the gyromagnetic tensor g and critical fields agree, within the experimental uncertainties, with those given in Ref. 33.

The determination of the polarization factors $P_{nv}(H)$, in principle obtained from an analysis of the intensity of

the modes, is very important to further test the limit of existing theories. By measuring systematically for each value of the field at two different scattering vectors $Q = (-0.5, 1, 0)$ (probing mainly the xy fluctuations) and $Q = (-2.1, 1, 0)$ (probing mainly the xz fluctuations), it has been possible to separate the various components involved in mode 3. Since our analysis has shown that only the y and z components play a role, the neutron intensity of mode 3 can be written as

$$I_3(Q) \propto f^2(Q) \left\{ \left[1 - \left(\frac{Q_z}{Q} \right)^2 \right] S_{3z} + \left[1 - \left(\frac{Q_y}{Q} \right)^2 \right] S_{3y} \right\}, \quad (11)$$

where $f(Q)$ is the magnetic form factor of Ni^{2+} ions and Q is the modulus of the scattering vector $Q = (Q_y, Q_z, 0)$. In the determination, we had to solve for each field value a simple system of two equations with two unknown variables, $S_{3z}(H)$ and $S_{3y}(H)$. The obtained values have been normalized to the previous value in zero field $S_{3z}(0)$. Figure 14 shows the experimental results of $S_{3z}(H)$ and $S_{3y}(H)$ for fields up to 100 kOe. Despite rather large error bars, our experimental data give some evidences for a slight decrease of the z component and a more convincing increase of the y component.

The field dependency of the normalized energy-integrated intensities for the two other modes are given in Fig. 15. Unfortunately, a complete determination of the polarization factors has not been performed for modes 1 and 2. Owing to the particular value of the scattering vector [$Q = (0.3, 1, 0)$], fluctuations along the x and y axes were mainly probed in these experiments, whereas the fluctuations along the z axis were almost suppressed by the geometrical factor $1 - (Q_z/Q)^2$. Quite similar to the previous case, we have, in fact, measured the total

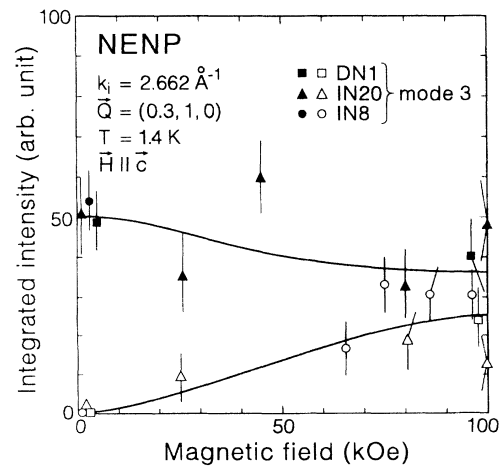


FIG. 14. Field dependence of the intensity integrated in energy at $q = \pi$ associated with mode 3, for a temperature $T = 1.4$ K. The solid lines are calculated from the polarization factors given in Ref. 38. The open symbols ($\circ, \triangle, \square$) are the experimental points for S_{3y} , while the solid symbols correspond to S_{3z} .

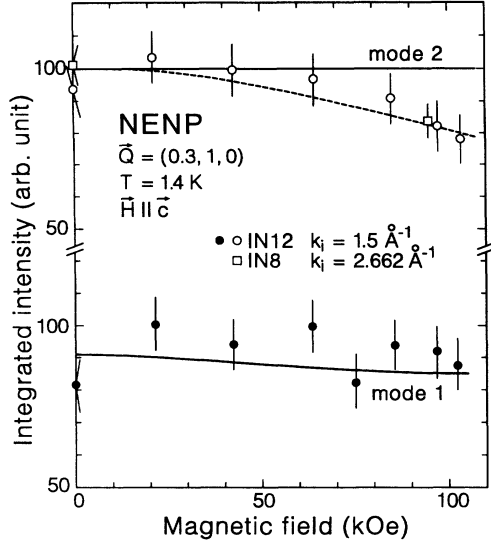


FIG. 15. Field dependence of the intensity integrated in energy at $q = \pi$ associated with modes 1 (solid circles) and 2 (open symbols) for a temperature $T = 1.4$ K. The solid lines correspond to the Affleck's theory described in Ref. 38. The dashed line is a fit to an empirical relation discussed in the text.

quantities $S_n(H) \approx S_{nx}(H) + S_{ny}(H)$ (with $n = 1, 2$) at the antiferromagnetic point, without possibility to separate the x and y components. As it can be seen in Fig. 15, S_1 (which is associated with the mode that softens) is very weakly field dependent. In contrast, S_2 (which is associated with a mode roughly constant in energy) is found to decrease with increasing field. This decrease (typically of order of 20% at $H = 100$ kOe) has been observed from measurements performed on thermal neutron spectrometers as well as cold-neutron spectrometers. Therefore, this effect is expected to be real.

We have analyzed our experimental data from the expressions of the polarization factors P_{1y} , P_{1z} , P_{2x} , P_{3y} , and P_{3z} at $q = k_{AF}$ obtained by Affleck³⁸ within the framework of the free boson field theory. The solid lines in Figs. 14 and 15 have been calculated from the theoretical results of Ref. 38, according to the following relations:

$$\begin{aligned} S_{1y}(H) &\approx S_{1y}(0) \cdot P_{1y}(H), \\ S_{2x}(H) &\approx S_{2x}(0), \\ S_{3y}(H) &\approx S_{1y}(0) \cdot P_{3y}(H), \\ S_{3z}(H) &\approx S_{3z}(0) \cdot P_{3z}(H), \end{aligned} \quad (12)$$

with the parameters $S_{1y}(0) \approx 90$, $S_{2x}(0) \approx 100$, and $S_{3z}(0) \approx 50$ previously determined from the zero-field experiments (see Sec. III A). The polarization factor $P_{1z}(H)$ is expected to take very small values, even in high field (typically $P_{1z} \approx 0.06$ for $H \approx 100$ kOe), preventing further determinations of $S_{1z}(H)$ by INS. Our experimental data on modes 1 and 3 are in surprisingly good agreement with the predictions of Affleck.³⁸ Concerning mode 2, the field-theory treatment predicts very weak

field dependencies,^{38,52} which cannot explain the non-negligible decrease observed in the component $S_{2x}(H)$ above 50 kOe. A better description of the experimental data can be obtained from the empirical relation

$$S_{2x}(H) \approx S_{2x}(0) / \sqrt{1 + (H/H_c^x)^2}.$$

The dashed line in Fig. 15 represents the best fitting to this relation with a parameter $H_c^x \approx 130$ kOe, roughly equal to the critical field. We have attributed this unexpected behavior to a possible field dependence of the correlation length ξ_x . More generally, ξ_y and ξ_z are also expected to vary under field, although quantitative theoretical results are rather scarce. Following the same kind of analysis performed on the data with the field parallel to the chain, it is possible to obtain information on the field dependencies of the correlation lengths ξ_x and ξ_y . From the sum rules previously mentioned,^{48,54} it is easy to obtain the following relations between the various parameters ξ_v , P_{nv} , and $\xi_{nv} = \kappa_{nv}^{-1}$:

$$\begin{aligned} \xi_x &= P_{1x}\xi_{1x} + P_{2x}\xi_{2x} + P_{3x}\xi_{3x}, \\ \xi_y &= P_{1y}\xi_{1y} + P_{2y}\xi_{2y} + P_{3y}\xi_{3y}, \\ \xi_z &= P_{1z}\xi_{1z} + P_{2z}\xi_{2z} + P_{3z}\xi_{3z}. \end{aligned} \quad (13)$$

From Eqs. (13) we can deduce a very simple relation expressing the sum $\xi_x + \xi_y$ as a function of the measured quantities S_1 , S_2 , and S_{3y} :

$$\xi_x + \xi_y \propto S_1(k_{AF}) + S_2(k_{AF}) + S_{3y}(k_{AF}) + P_{3x}\xi_{3x}. \quad (14)$$

Except the last term (absent in Affleck's theory), all the other terms have been determined in the present experiments. From our experimental data we have found that the total intensity associated with the in-plane fluctuations, namely $S_{xy} = S_1 + S_2 + S_{3y}$, was roughly independent of field within the error bars, with a value equal to 200 ± 10 (typically $S_{xy} \approx 190$ at $H = 0, 205$, at 40 kOe and 200 at 100 kOe). This implies, neglecting the last term in (14), that the quantity $\xi_x + \xi_y$ is experimentally more or less constant, at least up to about $0.7H_c^x$. Our experimental data can be understood if, in increasing field, the correlation length ξ_x is slightly decreasing, while the correlation length ξ_y is increasing. A typical order of magnitude for the relative variations at 100 kOe is 20% [typically $\xi_x \approx 0.8\xi_{xy}(0)$ and $\xi_y \approx 1.2\xi_{xy}(0)$]. In fact, such results are reminiscent to those obtained a long time ago for the classical easy-plane antiferromagnetic chain under a magnetic field applied along the x -axis. As shown by Villain,⁵³ within this configuration the correlation lengths ξ_x and ξ_y are given in a first approximation by linear relations in the reduced variable $u = (g_x \mu_B H / 4kT)^2$:

$$\begin{aligned} \xi_x &\approx (1 - u)\xi_0, \\ \xi_y &\approx (1 + u)\xi_0, \end{aligned} \quad (15)$$

where $\xi_0 \approx 2|J|S^2/kT$ is the correlation length of the classical 1D planar antiferromagnet in zero field. It is easy to verify that to the order $O(u^2)$ we have also the relation $\xi_x(H) + \xi_y(H) \approx 2\xi_0$, which is constant for a given tem-

perature. In the Haldane-gap problem, the above relations seems to apply quantitatively for the xy fluctuations with the substitution $u \approx \frac{1}{2}(H/H_c^x)^2$. In other words, the quantum fluctuations play the role of thermal fluctuations. We emphasize the strong difference in the values of the prefactors A_v when the field is applied along the chain ($A_{xy} \approx 2.8$) or perpendicular to the chain ($A_{x,y} \approx 0.5$). Experimentally, for the same ratio H/H_c^x , we have found a relative increase of ξ_y of about five to six times larger for the former field configuration. A probable explanation could originate from the completely different symmetries (xy -like or Ising-like, respectively) induced by the field. However, we have to mention that our experimental results are not consistent with the theoretical predictions given in Ref. 50, which seem to indicate the opposite effect. Undoubtedly, more precise calculations are needed to clarify this point. On the experimental side, more *direct* determinations under field of the correlation lengths ξ_x , ξ_y , and ξ_z appears urgent. Again the use of polarized neutrons should be a unique (but nontrivial) way to separate unambiguously the x and y contributions.

V. CONCLUSION

We have described exhaustive inelastic-neutron-scattering experiments on the nearly one-dimensional system with orthorhombic anisotropy NENP. Our experimental results are in excellent quantitative agreement with most theoretical predictions for the $S=1$ anisotropic antiferromagnetic chain. In particular, the observed values of the gaps are well understood from theoretical calculations, both in zero and applied field. Also, the finite value of the correlation length and the absence of long-range ordering at $T=0$ are quantitatively verified in our neutron-scattering data. The only point that is not well explained concerns the field dependencies of the vari-

ous structure factors. Although more experimental results seem necessary, especially to fully determine the polarization of the various modes, the present data show that a complete analysis requires more precise theoretical calculations of the components $S_{\alpha\alpha}(q, \omega)$ of the structure factor. In particular, such a theory should be able to give realistic expressions for the field dependency of the polarization factors and correlation lengths in the intermediate field range below H_c . Experimental studies of both the ground state and the excited states around and above H_c are expected to be very important for the understanding of such systems. Above H_c , the pure 1D-HAF system is expected to recover a more conventional gapless ground state at $T=0$, *without* long-range magnetic ordering but with an infinite correlation length.^{49,50} The experimental system should exhibit a 3D phase transition toward a true long-range ordering, induced by the weak interchain coupling J' , at a *finite temperature*.³⁷ We believe that such structural studies above H_c are feasible using neutron diffraction, with the field parallel to the chain. As far as the magnetic excitation spectrum above H_c is concerned, inelastic-neutron-scattering experiments seem *definitively impossible* using conventional three-axis spectrometers.

ACKNOWLEDGMENTS

We would like to thank J. Olivier and J. C. Ragazoni for their technical assistance in cryogenics, I. Affleck, J. P. Boucher, D. Grempel, S. V. Meshkov, and M. Verdaguer for numerous and illuminating discussions. Special thanks are due to O. Golinelli, Th. Jolicoeur, and R. Lacaze for their constant interest in the neutron-scattering results. Finally, we are indebted to B. Fak for a critical reading of the manuscript. Institut d'Electronique Fondamentale is Unité de Recherche Associée au CNRS No. 022.

*Permanent address: Kapitza Institute for Physical Problems, ulista Kosygina 2, 117334 Moscow, Russia.

¹F. D. M. Haldane, Phys. Lett. **93A**, 464 (1983); Phys. Rev. Lett. **50**, 1153 (1983).

²J. Des Cloiseaux and J. J. Pearson, Phys. Rev. **128**, 2131 (1962).

³G. Müller, H. Beck, and J. C. Bonner, Phys. Rev. Lett. **43**, 75 (1979).

⁴T. Yamada, Prog. Theor. Phys. Jpn. **41**, 880 (1969).

⁵I. Affleck, in *Fields, Strings and Critical Phenomena*, edited by E. Brézin and J. Zinn-Justin (North-Holland, Amsterdam, 1990), p. 563; J. Phys. Condens. Matter **1**, 3047 (1989).

⁶R. Botet and R. Jullien, Phys. Rev. B **27**, 613 (1983).

⁷R. Botet, R. Jullien, and M. Kolb, Phys. Rev. B **30**, 215 (1984).

⁸M. P. Nightingale and H. W. J. Blöte, Phys. Rev. B **33**, 659 (1986).

⁹T. Sakai and M. Takahashi, Phys. Rev. B **42**, 1090 (1990); **42**, 4537 (1990).

¹⁰K. Nomura, Phys. Rev. B **40**, 2421 (1989).

¹¹O. Golinelli, Th. Jolicoeur and R. Lacaze, Phys. Rev. B **45**, 9798 (1992); **46**, 10 854 (1992); J. Phys. Condens. Matter **5**, 1399 (1993).

¹²S. V. Meshkov, Phys. Rev. B **48**, 6167 (1993).

¹³W. J. L. Buyers, R. Morra, R. L. Armstrong, M. J. Hogan, P. Gerlach, and K. Hirakawa, Phys. Rev. Lett. **56**, 371 (1986).

¹⁴R. M. Morra, W. J. L. Buyers, R. L. Armstrong, and K. Hirakawa, Phys. Rev. B **38**, 543 (1988).

¹⁵Z. Tun, W. J. L. Buyers, R. L. Armstrong, K. Hirakawa, and B. Briat, Phys. Rev. B **42**, 4677 (1990).

¹⁶M. Steiner, K. Kakurai, J. K. Kjems, D. Petitgrand, and R. Pynn, J. Appl. Phys. **61**, 3953 (1987).

¹⁷K. Kakurai, M. Steiner, R. Pynn, and J. K. Kjems, J. Phys. Condens. Matter **3**, 715 (1991).

¹⁸I. Affleck, Phys. Rev. Lett. **62**, 474 (1989); **65**, 2477 (1990).

¹⁹H. Mutka, C. Payen, P. Molinie, J. L. Soubeyrou, P. Colom-bet, and A. D. Taylor, Phys. Rev. Lett. **67**, 497 (1991); Physica B **180-181**, 197 (1992).

²⁰A. Meyer, A. Gleizes, J. Gired, M. Verdaguer, and O. Kahn, Inorg. Chem. **21**, 1729 (1992).

²¹J. P. Renard, M. Verdaguer, L. P. Regnault, W. A. C. Erkelens, J. Rossat-Mignod, and W. G. Stirling, Europhys. Lett. **3**, 949 (1987).

²²O. Avenel *et al.*, Phys. Rev. B **46**, 9655 (1992).

- ²³Y. Ajiro, T. Goto, H. Kikuchi, T. Sakakibara, and T. Inami, *Phys. Rev. Lett.* **63**, 1424 (1989).
- ²⁴K. Katsumata, H. Hori, T. Takeuchi, M. Date, A. Yamagishi, and J. P. Renard, *Phys. Rev. Lett.* **63**, 86 (1989).
- ²⁵J. P. Renard, M. Verdager, L. P. Regnault, W. A. C. Erkelens, J. Rossat-Mignod, J. Ribas, W. G. Stirling, and C. Vettier, *J. Appl. Phys.* **63**, 3538 (1988).
- ²⁶L. P. Regnault, J. Rossat-Mignod, and J. P. Renard, *J. Magn. Magn. Mater.* **104-107**, 869 (1992).
- ²⁷L. P. Regnault, C. Vettier, J. Rossat-Mignod, and J. P. Renard, *Physica B* **156-157**, 247 (1989); **180-181**, 188 (1992).
- ²⁸S. Ma, C. Broholm, D. H. Reich, B. J. Sternlieb, and R. W. Erwin, *Phys. Rev. Lett.* **69**, 3571 (1992).
- ²⁹P. Gaveau, J. P. Boucher, L. P. Regnault, and J. P. Renard, *Europhys. Lett.* **12**, 647 (1990).
- ³⁰T. Goto, N. Fujiwara, T. Kohmoto, and S. Maegawa, *J. Phys. Soc. Jpn.* **59**, 1135 (1990); *Phys. Rev. B* **45**, 7837 (1992).
- ³¹N. Fujiwara, T. Goto, S. Maegawa, and T. Kohmoto, *Phys. Rev. B* **47**, 11 860 (1993).
- ³²M. Date and K. Kindo, *Phys. Rev. Lett.* **65**, 1659 (1990).
- ³³L. C. Brunel, T. M. Brill, I. Zaliznyak, J. P. Boucher, and J. P. Renard, *Phys. Rev. Lett.* **69**, 1699 (1992).
- ³⁴W. Lu, J. Tuchendler, M. von Ortenberg, and J. P. Renard, *Phys. Rev. Lett.* **67**, 3716 (1991).
- ³⁵W. Palme, H. Kriegestein, B. Lüthi, T. M. Brill, T. Yosida, and M. Date, *Int. J. Mod. Phys. B* **7**, 1016 (1993).
- ³⁶B. J. Sternlieb, L. P. Le, G. M. Luke, W. D. Wu, Y. J. Uemura, T. M. Riseman, J. H. Brewer, Y. Ajiro, and M. Mekata, *J. Magn. Magn. Mater.* **104-107**, 801 (1992).
- ³⁷T. Kobayashi, Y. Tabuchi, K. Ayama, Y. Ajiro, T. Yosida, and M. Date, *J. Phys. Soc. Jpn.* **61**, 1772 (1992).
- ³⁸I. Affleck, *Phys. Rev. B* **41**, 6697 (1990); **46**, 9002 (1992).
- ³⁹A. M. Tsvelik, *Phys. Rev. B* **42**, 10 499 (1990).
- ⁴⁰O. Golinelli, Th. Jolicœur, and R. Lacaze, *J. Phys. Condens. Matter* **5**, 7847 (1993).
- ⁴¹I. Affleck (unpublished); D. Grempel (private communication).
- ⁴²I. Affleck, *Phys. Rev. Lett.* **62**, 474 (1989).
- ⁴³Y. A. Kosevich and A. V. Chubukov, *Sov. Phys. JETP* **64**, 654 (1986).
- ⁴⁴T. Delica, K. Kopinga, H. Leschke, and K. K. Mon, *Europhys. Lett.* **15**, 55 (1991).
- ⁴⁵M. Takahashi, *Phys. Rev. Lett.* **62**, 2313 (1989).
- ⁴⁶G. Gomez-Santos, *Phys. Rev. Lett.* **63**, 790 (1989).
- ⁴⁷I. Affleck and R. A. Weston, *Phys. Rev. B* **45**, 4667 (1992).
- ⁴⁸J. Deisz, M. Jarrell, and D. L. Cox, *Phys. Rev. B* **42**, 4869 (1990).
- ⁴⁹T. Sakai, and M. Takahashi, *Phys. Rev. B* **44**, 10 385 (1991); *J. Phys. Soc. Jpn.* **62**, 750 (1993).
- ⁵⁰I. Affleck, *Phys. Rev. B* **43**, 3215 (1991).
- ⁵¹L. P. Regnault, I. Zaliznyak, and S. V. Meshkov, *J. Phys. Condens. Matter* **5**, L677 (1993).
- ⁵²S. V. Meshkov (private communication).
- ⁵³J. Villain, *J. Phys. (Paris)* **35**, 27 (1974).
- ⁵⁴P. C. Hohenberg and W. F. Brinkman, *Phys. Rev. B* **10**, 128 (1974).

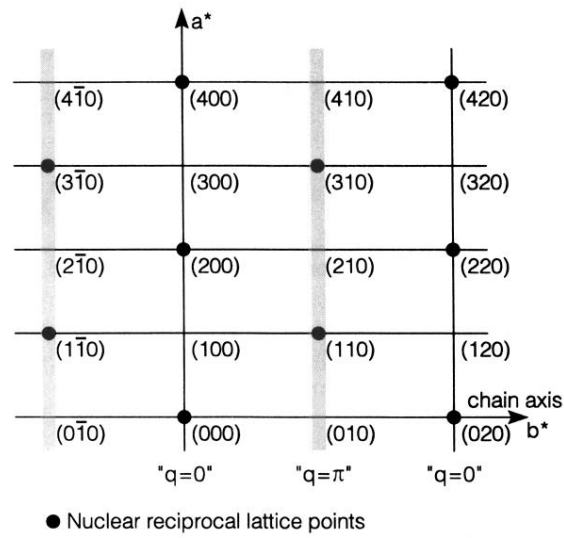


FIG. 1. The (a^*, b^*) plane of the reciprocal lattice. The shaded areas denote the positions of one-dimensional antiferromagnetic planes ($q = \pi$).